Macromolecules
ARTICLE

Macromolecules **2010**, *43*, 4261–4267 **4261**
DOI: 10.1021/ma1000817

Cubic to Hexagonal Phase Transition Induced by Electric Field

Fernando C. Giacomelli,*,† Nádya P. da Silveira,‡ Frédéric Nallet,§ Petr Černoch,⊥ Miloš Steinhart,⊥ and Petr Štěpánek*,⊥

†*Centro de Ciências Naturais e Humanas, Universidade Federal do ABC, Rua Santa Adélia 166, 09210-170, Santo André - SP, Brazil,* ‡*Institute of Chemistry, Universidade Federal do Rio Grande do Sul, Av. Bento Gonçalves 9500, 91501-970 Porto Alegre, Brazil,* §*Centre de Recherche Paul-Pascal, CNRS, 115 Avenue du Docteur-Schweitzer, 33600 Pessac, France, and* ⊥*Institute of Macromolecular Chemistry, Heyrovský Sq. 2, 162 06 Prague 6, Czech Republic*

Received January 12, 2010; Revised Manuscript Received April 6, 2010

ABSTRACT: The possibility of electric field induced phase transitions in soft matter systems was studied by means of small-angle X-ray (SAXS) and neutron (SANS) scattering measurements. By dissolving a diblock copolymer PS-*b*-PEP (polystyrene-*block*-poly(ethylene-*co*-propylene)) in a mixture of cyclohexane (CH) and dimethylformamide (DMF), it was possible to create a liquid 3D cubic structure in which spherical microdomains of DMF were embedded into a liquid CH (major component) matrix with the liquid−liquid interfaces covered by PS-*b*-PEP diblock copolymer chains. When sited under an external electric field, the experimental SAXS and SANS results revealed that the initial self-organized 3D cubic structure is converted into an hexagonal arrangement. The order-to-order transition was reached by the application of a relatively low dc electric field, ∼1.25 kV/mm. The electric field generates dipole moments in DMF-rich spherical microdomains that are deformed and further interconnected, leading to the formation of the hexagonal packed cylinders. The electric field strength E_t needed to induce such transition depends on the magnitude of the generated dipole moment in the DMF-rich spherical microdomains and hence depends on their size and dielectric contrast irrespective of the surrounding liquid. The latter must have the lower dielectric constant for the transition to occur. E_t also increases with increasing block copolymer concentration. The chain statistics does not change at the transition and always corresponds to that of a polymer in good solvent. The HEX-cylinders phase developed under external electric field is unstable, and as soon as the field is switched off, the cylinders undergo an order-to-order transition back to the cubic phase. Finally, another HEX-cylinders phase thermodynamically stable without electric field was created by dissolving a PS-*b*-PI diblock copolymer (polystyrene-*block*-polyisoprene) in a CH−DMF mixture. In this last case, the structure essentially does not feel the presence of an electric field of the same magnitude.

Introduction

Application of external electric fields has been shown to be an efficient method for controlling the microdomain orientation of soft structures[1,2] as well as for tuning morphologies of polymer blends[3,4] and dimensions of microphase-separated nanoscopic arrangements.[5,6] In particular, the behavior of microphase-segregated block copolymers under external electric field has been increasingly investigated mainly by means of small-angle X-ray (SAXS) and neutron (SANS) scattering measurements. Scattering techniques are definitely powerful to probe the structure of self-organized nanostructured systems. Herein, we show that application of an external electric field can induce an order-to-order transition in a self-organized block copolymer solution: specifically, in a solution of a diblock copolymer dissolved in a mixture of partially miscible solvents a cubic to hexagonal phase transition can be induced.

Block Copolymers in Partially Miscible Solvents. A self-organization might be expected when an AB-type block copolymer is dissolved in inversely selective partially miscible solvents (i.e., solvents in which one block is soluble in one solvent and the other is insoluble and vice versa for the other solvent). When the two neat solvents are partially miscible, the phase diagram (temperature, composition) exhibits a coexistence curve. For temperatures below the coexistence curve, the block copolymer chains are driven to the liquid−liquid interface due to the favorable interaction of the solvent−block pairs, and depending on a number of parameters, thermodynamically stable microdomains may be obtained in which "droplets" of the minor solvent are embedded in a matrix composed by the major solvent; the liquid−liquid interfaces are stabilized by the block copolymer chains forming a brush as schematically represented in Figure 1. Theoretically, it has been suggested that depending on the symmetry of the block copolymer chains, copolymer concentration, solvent composition, temperature, and other thermodynamic parameters, various ordered structures may be achieved, exhibiting in particular a lamellar, cylindrical, or spherical morphology.[7,8] Experimentally, the formation of long-range structures arranged in a cubic lattice or as hexagonal packed cylinders was recently observed in CH−DMF mixtures and polystyrene-*b*-polybutadiene or polystyrene-*b*-poly(ethylene propylene) at the liquid−liquid interfaces.[9] For the binary solvent mixture CH−DMF the coexistence curve has an upper critical solution temperature of 48 °C at a volume fraction $\phi_{DMF} = 0.38$.

Electric Field Effects on Soft Matter Systems. The effect of electric fields on the dynamics and structure of soft matter systems has been receiving increasing attention. Currently, we have focused on the dynamics of nanoscale self-assemblies under external electric field by means of

*Corresponding authors: e-mail stepan@imc.cas.cz, Tel +420 2 96809211 (P.Š.); e-mail fernando.giacomelli@ufabc.edu.br, Tel +55 11 2936 0416 (F.C.G.).

Published on Web 04/14/2010

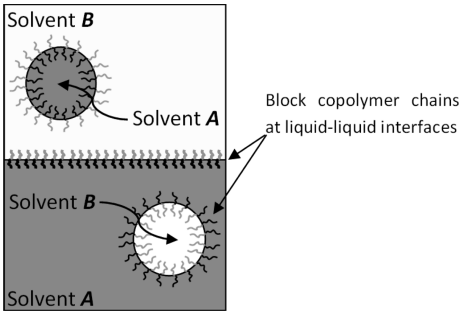

Figure 1. Representation of a diblock copolymer dissolved in inversely selective partially miscible solvents A and B.

dynamic light scattering measurements.[10−12] Simultaneously, the alignment of block copolymer microdomains in concentrated solutions by using electric field strengths ~1−2 kV mm^{-1} has been extensively investigated by Krausch et al.[1,2,13−15] They deeply explored the microscopic mechanisms of alignment and the influence of the initial order[16] and dielectric contrast[17] on the kinetics of microdomain orientation.

The alignment of block copolymer microdomains organized in thin films was also demonstrated to be achievable. Thin films alignment is controlled by the applied electric field,[14,18,19] interfacial energies (due to the influence of the substrate),[20−22] and thickness.[23] In any case, however, the covalently bonded blocks must possess a sufficient dielectric contrast $\Delta\varepsilon$ for the alignment to be physically possible. It was experimentally demonstrated that lamellar and cylindrical microdomains (in symmetric and asymmetric PS-*b*-PMMA block copolymer thin films respectively) can be oriented macroscopically parallel to the applied electric field ($E \sim$ 30 kV/mm).[18,19] This effect is much more easily reachable by modifying the substrate surface, thereby lowering the interfacial interactions,[24] or by the formation of lithium−PMMA complexes, thereby enhancing the dielectric contrast between the two segregated domains.[25] The electric field can also induce sphere-to-cylinder transition in block copolymer thin films.[26] Russell et al. showed that random packed spherical microdomains in PS-*b*-PMMA thin films can be deformed to ellipsoids and further interconnected to form cylindrical microdomains.[27]

Essentially, the driving force in all processes detailed above is intrinsically related to the dielectric contrast present in the system. The electric field is able to influence the dynamics and/or structure of soft matter samples if a sufficient dielectric contrast exists. Herein, we wish to demonstrate experimentally the possibility to induce phase transitions in soft matter materials via the application of external electric field. A cubic arrangement was developed when PS-*b*-PEP was dissolved in a mixture of cyclohexane (CH) and dimethylformamide (DMF). Since the neat solvents are immiscible, at room temperature spherical microdomains of DMF are embedded in a liquid CH matrix with the liquid−liquid interfaces covered by diblock copolymer chains. Under external electric field, the DMF spherical microdomains are deformed and interconnected, leading to the formation of DMF cylinders hexagonally packed. Because of the huge dielectric contrast between the cyclohexane liquid matrix ($\varepsilon_{CH} = 2.0$) and DMF-containing spherical microdomains ($\varepsilon_{DMF} = 38.0$), an electric field strength ~1.25 kV/mm was fairly enough to induce the phase transition.

Materials and Methods

Samples Preparation. Two block copolymer samples were used: the first one labeled SV-50 (Shellvis 50) is a commercial product of the Shell Co., and it is a diblock copolymer polystyrene-*b*-polyisoprene in which the polyisoprene block was fully hydrogenated after polymerization, i.e., polystyrene-*b*-poly(ethylene-*co*-propylene). Herein, it is labeled PS-*b*-PEP. The polymer has molecular weight (M_w = 96 000 g/mol), polydispersity (M_w/M_n = 1.02), and polystyrene weight fraction (w_{PS} = 0.43). The second one, labeled PS-*b*-PI, is a diblock copolymer polystyrene-*b*-polyisoprene (M_w = 165 000 g/mol, M_w/M_n = 1.06, and w_{PS} = 0.76) purchased from Polymer Source, Inc., Canada.

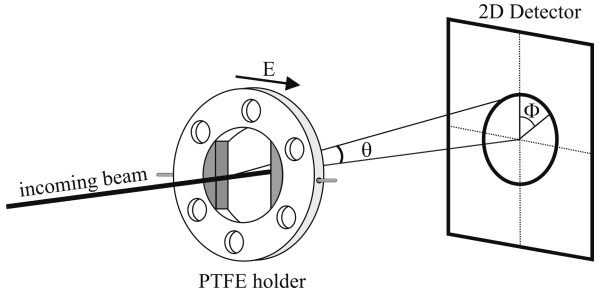

Figure 2. Schematic representation of the home-built capacitor used in the experiments.

The solvents cyclohexane (CH) and dimethylformamide (DMF) were of analytical grade, anhydrous, and in the fully deuterated form. They were purchased from Chemotrade (Leipzig) and used as received. The block copolymer solutions were prepared by dissolving the dry samples into appropriate mixture of solvents CH and DMF into commercial cuvettes and flame-sealed. Afterward, the solutions were homogenized overnight in an oven at 60 °C (i.e., above the phase separation temperature of the neat solvents).[9] Lastly, the samples were left at room temperature for at least 1 week to achieve the equilibrium structures.

Electric Field Setup. The dc electric field was applied through the samples by using a home-built capacitor. The setup is schematically represented in Figure 2.

The viscous samples were loaded into a 2 mm thick PTFE holder and sealed by two 25 μm thick mica (SAXS) or 1 mm thick quartz (SANS) windows. Two semicircular gold electrodes (in gray in Figure 2) were attached to the PTFE holder separated by 1.6 mm (SAXS) or 8 mm (SANS). It is worth to mention that even though the electrodes separation was different, the electric field intensity reached in SAXS and SANS measurements was the same, which was set up by using a safety 30 kV high-voltage cable attached to an EMCO high-voltage power supply. During all the measurements, the applied voltage and the current density were carefully monitored using a standard circuit. The current density, independently of the applied voltage, was always negligible, suggesting that the conductivity of the samples is insignificant. This is reasonable since they were composed mainly by cyclohexane.

SAXS Measurements. The SAXS measurements were performed at the high brilliance beamline ID02 of the European Synchrotron Radiation Facility (ESRF). The wavelength (λ) of the incoming beam was set to 0.1 nm, and the sample-to-detector distance was chosen as 2 or 5 m to cover the targeted q range, being $q = (4\pi/\lambda)\sin(\theta/2)$ (θ is the scattering angle). The collimated beam crossed the capacitor (Figure 2) and was scattered to an X-ray image intensified low noise CCD (FReLoN) detector placed in an evacuated flight tube. The images were found to be isotropic, and the treatment has been made taking into account the 360° azimuthal scan. Since CH and DMF are not miscible at room temperature, the resulting $I(q)$ vs q curves were corrected by the subtraction of the scattering of CH−DMF mixtures (with the same composition of the samples) measured at 60 °C (above the phase separation temperature of the neat solvents). Furthermore, $I(q)$ was recalculated in absolute scale using Lupolen as standard.

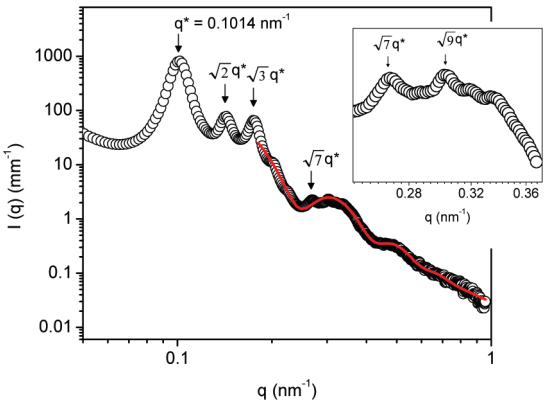

Figure 3. $I(q)$ vs q SAXS profile for 10% w/w PS-*b*-PEP dissolved in the partially miscible solvents CH−8% DMF at $E = 0$ kV/mm.

SANS Measurements. Small-angle neutron scattering experiments were performed at CEA-Saclay on the spectrometer PAXY of the Laboratoire Léon-Brillouin. Measurements were performed with a 128 × 128 multidetector (pixel size 0.5 × 0.5 cm^2), using a nonpolarized and monochromatic incident neutron beam. The sample-to-detector distance was chosen as 1 m, and the wavelength was $\lambda = 0.8$ nm (set by a velocity selector). Similar to the SAXS measurements, the 2D images were isotropic and azimuthally averaged to yield $I(q)$ vs q profiles. They were previously corrected by the background scattering and empty cell, normalized by the path length and transmission of the sample, and subtracted by the scattering of CH−DMF mixtures measured above the phase separation temperature of the neat solvents.

Results and Discussion

BCC-Spheres Cubic Lattice under External Electric Field. We performed a detailed investigation on the self-organization of diblock copolymers dissolved in partially miscible solvents and under an external electric field. A broad range of experimental conditions were investigated, namely, block copolymer nature and concentration, solvent composition, electric field strength, and initial configuration (cubic or hexagonal arrangement). Figure 3 reports the SAXS profile of 10% w/w PS-*b*-PEP dissolved in partially miscible solvents CH−8% DMF at $E = 0$ kV/mm.

As one can easily see, the main peak related to the structure factor of the self-organized system is located at $q^* = 0.1014$ nm^{-1}. There are also two secondary maxima at $2^{1/2}q^* = 0.1429$ nm^{-1} and $3^{1/2}q^* = 0.1755$ nm^{-1}. The presence of the $2^{1/2}q^*$ and $3^{1/2}q^*$ peaks suggests a long-range cubic structure. The face-centered-cubic arrangement can be ruled out since in such a case a secondary peak would appear at $(4/3)^{1/2}q^* = 0.1170$ nm^{-1}. Still more important is the weak scattering peak at $7^{1/2}q^* = 0.2677$ nm^{-1} (expanded in the top right of Figure 3), which is characteristic for a BCC (body-centered cubic) organization as opposed to a primitive cubic lattice. Therefore, one can conclude that the system starts as a structure of BCC-spheres. Since DMF is the minor component, it is straightforward to preview the formation of DMF-rich spherical microdomains embedded in a cyclohexane liquid matrix and the PS-*b*-PEP chains forming a brush at the liquid−liquid interfaces.

In dealing with BCC arrangements, the main scattering peak is related to the distance d between the scattering planes 110 (D_{110}) of the 3D structure (Figure 4, bottom). Therefore, the relation between a (cubic dimension) and q^* is given by

$$q^* = q_{110} = \frac{2\pi}{d} = \frac{2\pi\sqrt{2}}{a} \qquad (1)$$

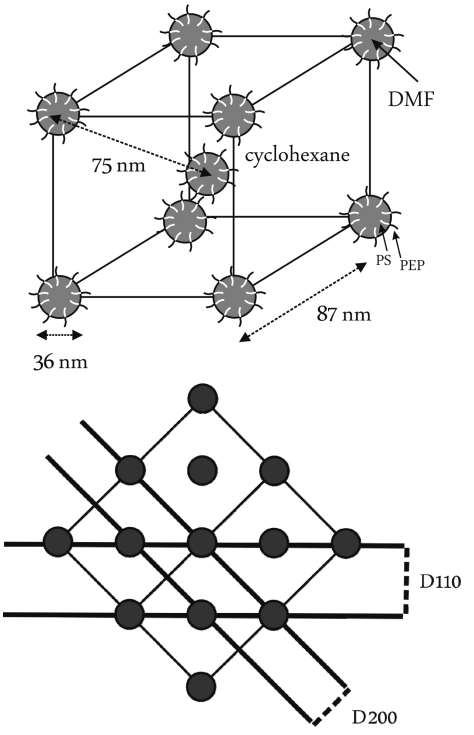

Figure 4. Schematic illustration showing the initial spatial arrangement of the microdomains for 10% w/w PS-*b*-PEP dissolved in CH−8% DMF at $E = 0$ kV/mm (top). Representation of a standard BCC-spheres structure and its main scattering planes (bottom).

At the high-q range, the form factor of the building objects dominates the scattering profile. As shown in Figure 3 (solid red line), it was possible to fit the high-q range of the SAXS profile by using the form factor of homogeneous spheres as

$$I(q) = V_p{}^2\Delta\sigma^2 P(q,R) = \left(\frac{4}{3}\pi R^3\Delta\sigma\right)^2\left(\frac{3[\sin(qR) - qR\cos(qR)]}{(qR)^3}\right)^2 \qquad (2)$$

with R being their radius. The fitting procedure led to $R = 18.0$ nm, and its polydispersity determined using the Schulz distribution was equal to $\sigma = 0.13$. Hence, the initial configuration of the 3D structure could be sketched (Figure 4, top).

The SAXS profile of the same sample was found to be completely different as soon as the electric field was switched to $E = 1.25$ kV mm^{-1} (Figure 5). The main peak shifts to $q^* = 0.1205$ nm^{-1}. Of essential meaning is the vanishing of the secondary maxima located at $2^{1/2}q^*$ and the remaining of a secondary reflection at $3^{1/2}q^* = 0.2061$ nm^{-1}. Such configuration is only compatible with a hexagonal arrangement. Therefore, we claim that the electric field was able to promote a phase transition in the system from a cubic to a hexagonal structure. The time scale for such transition is relatively fast (within the range of a few seconds).

The high-q range in Figure 5 could be fitted by using the form factor of long cylinders ($L \gg R$) with L being their length and R their radius as

$$I(q) = (\Delta\sigma\pi R^2)^2\left(\frac{2J_1(qR)}{qR}\right)^2 \qquad (3)$$

The fitting procedure led to $R = 13.4$ nm and $\sigma = 0.17$. This is in full agreement with the phase transition proposed.

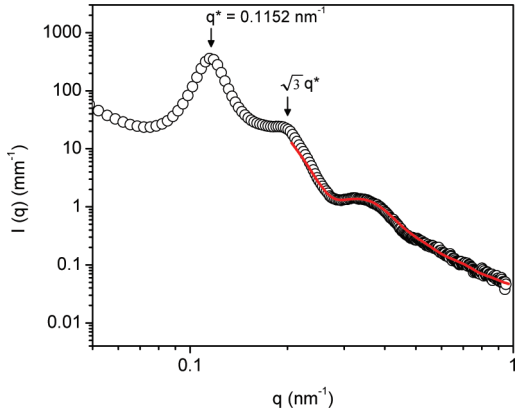

Figure 5. $I(q)$ vs q SAXS profile for 10% w/w PS-*b*-PEP dissolved in the partially miscible solvents CH−8% DMF and under external electric field ($E = 1.25$ kV/mm).

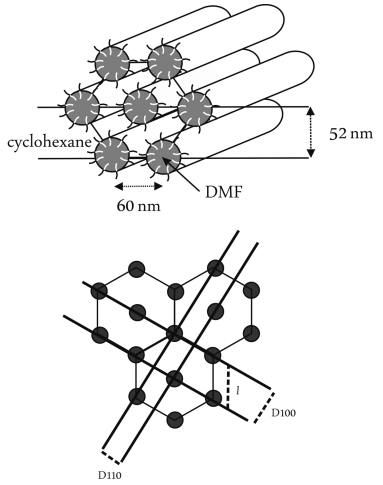

Figure 6. Schematic illustration showing the spatial arrangement of the microdomains for 10% w/w PS-*b*-PEP dissolved in CH−8% DMF at $E = 1.25$ kV/mm (top). Representation of a standard HEX-cylinders structure and its main scattering planes (bottom).

Considering the hexagonal structure, the main peak at $q^* = 0.1152$ nm^{-1} is related to the D_{100} distance. The D_{100} scattering planes are separated by $l3^{1/2}/2$, with l being the distance between the packed cylinders (Figure 6, bottom).

$$q^* = q_{100} = \frac{2\pi}{D_{100}} = \frac{4\pi}{l\sqrt{3}} \tag{4}$$

The secondary maxima at $3^{1/2}q^*$ is related to the distance between the D_{110} scattering planes, being $D_{110} = l/2$. Figure 6 portrays the configuration of the given system proposed based on the SAXS measurements under external electric field.

As determined, $R_{\text{cylinder}} < R_{\text{sphere}}$ and the cylinders have higher polydispersity. Furthermore, according to the fitting model, the length (L) of the cylinders is probably much longer than its radius, i.e., $L \gg 13.4$ nm, which is perfectly reasonable. The main scattering peak of the hexagonally packed cylinders structure appears at a higher q^* than that for the BCC-spheres. It means that the main scattering plane distance in the BCC-spheres is bigger than in the HEX-cylinders one ($D_{\text{BCC-110}} = 62$ nm $> D_{\text{HEX-100}} = 52$ nm).

Considering the interaction of electric fields with soft matter systems, the speculated mechanism responsible for the proposed transition is supposed to be linked to the generation of dipole moments in the DMF-rich microdomains.

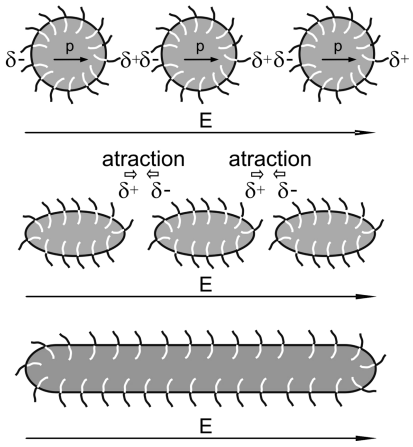

Figure 7. Schematic representation of the speculated transition from spheres to cylinders in the self-organized polymer system studied under external electric field.

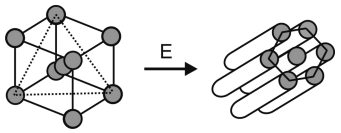

Figure 8. Schematic representation for the BCC-spheres to HEX-cylinders transition in the self-organized polymer system studied under external electric field. The dotted lines represent the [111] scattering plane of the BCC structure. The HEX-cylinder phase is supposed to be formed by the interconnection of the DMF-rich spherical microdomains through the direction normal to the 111 scattering plane under external electric field.

The induced dipole moment (p) can quantitatively be described for homogeneous spheres as[28]

$$p = 4\pi\varepsilon\varepsilon_0\beta R^3 E \tag{5}$$

wherein ε_0 is the permittivity of the free space (8.854×10^{-12} F m^{-1}) and ε is the dielectric constant of the surroundings (CH). The parameter β is a dielectric mismatch parameter that involves the dielectric constant of the DMF-rich microdomains and the cyclohexane-rich matrix. Since $\beta > 0$ (that is to say, $\varepsilon_{\text{DMF-domains}} > \varepsilon_{\text{CH-matrix}}$), the dipole moment acquired by the DMF-rich domains has the same direction as the electric field applied.[28] In such a case, the DMF domains attract each other or they can be deformed and further interconnect forming cylindrical microdomains, as sketched in Figure 7.

Therefore, the cylindrical microdomains grow in the direction of the applied electric field. It is supposed that the deformation and interconnection of the spherical microdomains take place toward the closest ones: it means in the direction normal to the D_{111} scattering plane of the BCC-spheres structure (as sketched in Figure 8). The phase transition from BCC-spheres to HEX-cylinders in such way is currently straightforward when induced by temperature changes in bulk block copolymers.[29−32]

Furthermore, it has been suggested theoretically that the cubic-to-hexagonal phase transition induced by electric field in block copolymer melts is thermodynamically favorable when the spherical microdomains are aligned along the [111] direction instead of the [100].[33] We have observed also that the BCC−HEX phase transition is fully reversible within the range of 1−2 min. As soon as we switched off the electric field, the BCC-spheres structure initially present was reformed, as shown by the reappearance of the three main

peaks at the low-q range of the SAXS profile and at well-defined positions q^*, $2^{1/2}q^*$, and $3^{1/2}q^*$ (not shown here). Such reversibility was also suggested theoretically by using cell dynamics simulation.[34] Equally interesting, the cubic-to-hexagonal phase transition was found to be reachable in this liquid−liquid self-organized system by using a relatively low electric field strength ($E \sim 1.25$ kV/mm), whereas sphere-to-cylinder transition on asymmetric PS-*b*-PMMA block copolymer thin films was only achievable by using $E \sim 40$ kV/mm.[27] Theoretically, even higher electric field was predicted to be needed to induce the given transition (~70 kV/mm).[5,33] Alternatively, Lyakhova et al.[35] by using a different theoretical approach estimated an electric field strength $E \sim 18$ kV/mm for a full spheres-to-cylinders transition on PS-*b*-PMMA at $T = 170$ °C ($\varepsilon_{PMMA} = 6.0$ and $\varepsilon_{PS} = 2.5$), which is a reasonable value once $E \sim 40$ kV/mm was experimentally proved to be enough.[27] Furthermore, although in the work of Leibler et al.[5] the BCC−HEX transition in PS-*b*-PMMA was calculated to be reachable at $E \sim 70$ kV/mm, they have claimed that such value can be reduced by the presence of dissociated ions in the block copolymer sample due to the ability of the free charges to diffuse in the hexagonal phase. It was theoretically demonstrated that dissociated ions are supposed to induce a BCC−HEX phase transition in PS-*b*-PMMA at $E \sim 6-10$ kV/mm, and the critical E value can still be tuned by the amount of free ions present. Russell et al. have comprehensively studied PS-*b*-PMMA thins films under external electric field, and they demonstrated experimentally that the formation of ionic complexes on PS-*b*-PMMA thin films was found to alter the critical electric field strength needed to induce the spheres-to-cylinders transition as well as the time scale of the kinetics due to the increase in $\Delta\varepsilon$ and the mediation of interfacial interactions.[36]

As exposed above, the experimental and theoretical contributions related to this field are mainly focused on PS-*b*-PMMA. In such system, the dielectric contrast ($\Delta\varepsilon$) comes from the two blocks ($\varepsilon_{PMMA} \sim 6.0$, $\varepsilon_{PS} \sim 2.5$, and $\Delta\varepsilon \sim 3.5$). On the other hand, in the current contribution, the dielectric contrast comes from the two solvents. Since such liquids have especially distinct dielectric constants ($\varepsilon_{DMF} \sim 38.0$, $\varepsilon_{CH} \sim 2.0$, and $\Delta\varepsilon \sim 36$), a much lower electric field strength is needed to induce the phase transition given that the electric field strength required is essentially dependent on the dielectric contrast. This is evidenced experimentally by our finding, $E \sim 1.25$ kV/mm.

Besides SAXS measurements discussed throughout the article, we have also performed SANS measurements in the same sample. Since we have used always fully deuterated solvents which have almost completely matched scattering length densities, the SANS scattering contrast does not come from the spherical or cylindrical objects embedded in the matrix solvent but only from the (nondeuterated) polymer chains observed on a homogeneous solvent background. In the q-range approximately above $q = 0.7$ nm^{-1} the scattered intensity $I(q)$ is predicted[37] to decay as $I(q) \sim q^{-a}$, where a is the inverse of the Flory exponent ν ($a = 1/\nu$) in the relation between the radius R and the molecular weight M of a polymer coil, $R \sim M^{\nu}$.

Figure 9 shows the high-q range SANS profile for 10% w/w PS-*b*-PEP dissolved in CH−8% DMF under electric field having different intensities as given in the figure legend. As the results suggest, within experimental errors no differences of the scattering curves were observed for values of the electric field up to 1.25 kV/mm. The high-q range of the spectra gives us information about the chains statistics. The slope a is practically constant, $a \sim 1.61$, yielding $\nu = 0.62$. This means that the extension of the chains at the liquid−liquid interfaces

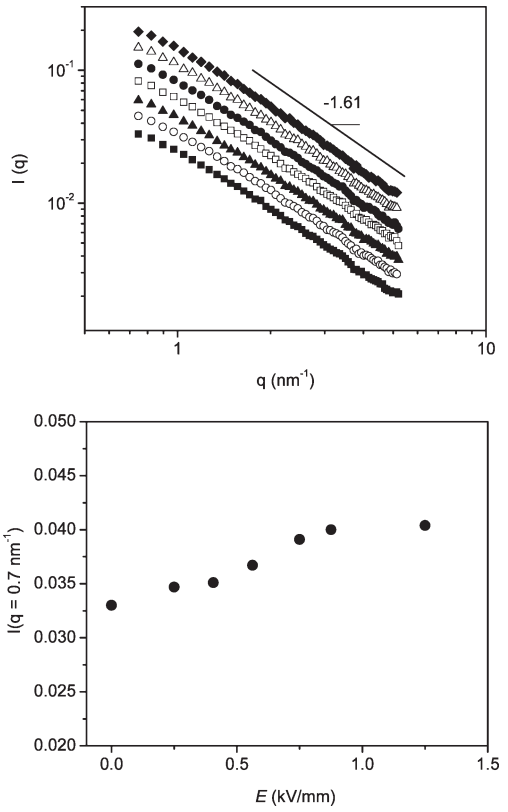

Figure 9. High-q range SANS profile for 10% w/w PS-*b*-PEP dissolved in CH−8% DMF under electric field having different intensities (■) 0, (○) 0.25, (▲) 0.44, (□) 0.55, (●) 0.75, (Δ) 0.88, and (◆) 1.25 kV/mm. The curves have been shifted vertically by 0.3 decade (top). Dependence on the intensity of the SANS curves at $q = 0.7$ nm^{-1} on the electric field E before been vertically shifted (bottom).

is independent of the presence of electric field. The chains simply cover the new interfaces generated by the electric field in the same way they have covered the original ones. That is plausible since the electric field has an effect because of the dielectric contrast between cyclohexane and DMF, and the polymer chains do not feel it. The intensity of the scattering curves at $q = 0.7$ nm^{-1} in Figure 9 before shifting them vertically increases by about 20% when the applied electric field increases from 0 to 1.25 kV/mm (Figure 9, bottom). Since the number of chains does not change, the source for such increase might be related to the fact that the total surface of the cylinders in the hexagonal arrangement is larger than the total surface of the spheres in the BCC structure.

Lastly, the electric field threshold E_t needed to induce the BCC−HEX transition was found to be dependent on the solvent composition and block copolymer concentration (Figure 10). As the amount of DMF increases, two additional factors are believed to influence E_t: (i) the changes in the phase coexistence boundaries between the BCC and HEX phases and (ii) the increase in the volume of the DMF microdomains which leads to an increase in the magnitude of the dipole moment generated since $p \sim R^3$ (eq 5). The influence of the copolymer concentration is even more pronounced, where a slight increase from 6% to 10% w/w PS-*b*-PEP led to an increase in E_t from 0.60 to 1.25 kV.

HEX-Cylinders Arrangement under External Electric Field. Figure 11 reports the SAXS profile at $E = 0$ kV/mm and $E = 1.85$ kV/mm for 7% w/w PS-*b*-PI dissolved in the partially miscible solvents CH−8% DMF. At $E = 0$ kV/mm (lower curve), the main scattering peak of the solution

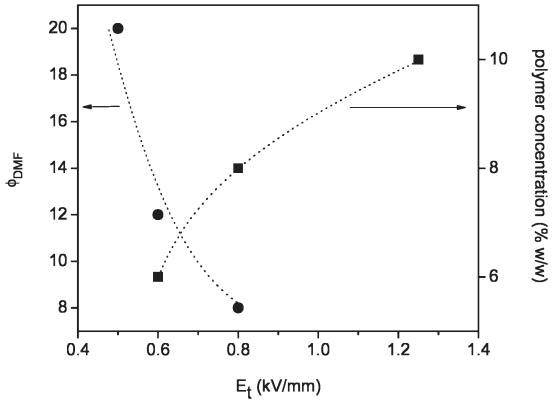

Figure 10. E_t dependence on ϕ_{DMF} ($c_{PS\text{-}b\text{-}PEP}$ = 8% w/w) and block copolymer concentration (ϕ_{DMF} = 8%) to induce the BCC-spheres to HEX-cylinders transition.

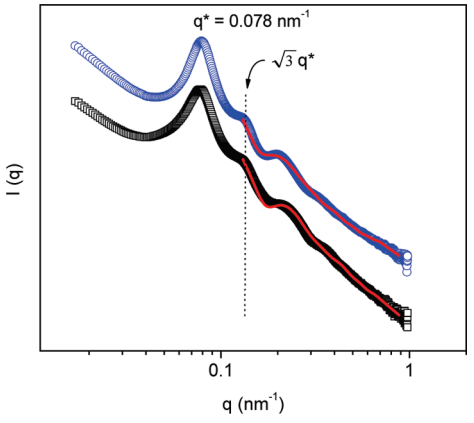

Figure 11. $I(q)$ vs q SAXS profile for 7% w/w PS-*b*-PI dissolved in CH−8% DMF at E = 0 kV/mm (open squares, lower curve) and E = 1.85 kV/mm (open circles, upper curve).

structure factor is located at $q^* = 0.078$ nm^{-1}. A secondary maxima is seen at $3^{1/2}q^* = 0.1337$ nm^{-1}. The absence of the corresponding peak at $2^{1/2}q^*$ shows that the system is initially self-organized in a HEX-cylinders arrangement. Previous small-angle neutron scattering (SANS) measurements in the same sample also suggests such arrangement.[9] Above E = 1.85 kV/mm, we could not avoid shortcuts between the electrodes. Nevertheless, as one can notice checking the upper and lower curves in Figure 11, the scattering profiles are roughly independent of the applied electric field.

The upper curve is y-shifted by 1 order of magnitude for better visualization. The structure factor of the self-organized polymer system is basically independent of the presence or not of an applied electric field, at least up to 1.85 kV/mm. We were able to detect only a slight difference in the high-q range of the scattering profile (form factor region). The solid red curves given in Figure 11 are the high-q range fittings of the scattering profiles using the long cylinder form factor (eq 3). The high-q range fitting procedures led to the following values at E = 0 kV/mm and E = 1.85 kV/mm: R = 21.8 nm, σ = 0.15 and R = 22.6 nm, σ = 0.17. It means that even under such high external electric field, the supposed hexagonal arrangement does not seem to be influenced by the external force. These results point out that the electric field is not able to induce a pronounced change in a hexagonal structure, such as it can do in a 3D-cubic arrangement.

Conclusions

We have shown experimentally that electric field can induce phase transitions in soft matter organized systems. A cubic to hexagonal rearrangement was proved to be reachable by the application of an electric field strength ~1.25 kV/mm starting from a cubic 3D structure self-formed from PS-*b*-PEP diblock copolymer dissolved in a mixture of cyclohexane and DMF. It is believed that such kind of transition might be possible in any similar system if the dielectric contrast between matrix and microdomains is sufficiently high and if the microdomains have higher dielectric constant than its surroundings.

The hexagonal cylinders developed under external electric field are unstable, and the reversibility of the order-to-order phase transition occurs within the range of 1−2 min. The electric field threshold E_t needed to induce the rearrangement depends on the induced dipole moment in the microdomains: it is mainly related to their size and dielectric contrast irrespective of the surroundings. E_t was found to be also dependent on the block copolymer concentration covering the liquid−liquid interfaces. On the other hand, a HEX-cylinders phase thermodynamically stable at E = 0 kV/mm essentially does not feel the presence of an electric field of the same magnitude.

Finally, it is worth to say that currently we are working on the other side of the CH−DMF phase diagram (in which the matrix is formed by the higher dielectric constant component—DMF and having CH microdomains embedded). As soon as we reach the optimal conditions to obtain the self-organized 3D structures, they will be also studied under external electric field. Thus, we will be able to compare results for systems loading distinct β parameters (i.e., distinct positions of the higher dielectric constant component).

Acknowledgment. We acknowledge support by the Grant Agency of the Czech Republic (Grant P208/10/1600) and ESRF (Proposal SC-2667) for beam time that was supported also by the Czech Ministry of Education (grant INGO LA 287) and J. Gummel for assistance with the SAXS measurements. The Laboratoire Leon Brillouin is acknowledged for neutron time and L. Noirez for assistance during SANS measurements. F.C.G. and N.P.S. thank CNPq for the financial support.

References and Notes

(1) Boker, A.; Knoll, A.; Elbs, H.; Abetz, V.; Muller, A. H. E.; Krausch, G. *Macromolecules* **2002**, *35*, 1319–1325.
(2) Boker, A.; Elbs, H.; Hansel, H.; Knoll, A.; Ludwigs, S.; Zettl, H.; Urban, V.; Abetz, V.; Muller, A. H. E.; Krausch, G. *Phys. Rev. Lett.* **2002**, *89*, 1355021–4.
(3) Venugopal, G.; Krause, S.; Wnek, G. E. *J. Polym. Sci., Polym. Lett.* **1989**, *27*, 497–501.
(4) Venugopal, G.; Krause, S.; Wnek, G. E. *Polym. Prepr.* (*Am. Chem. Soc., Div. Polym. Chem.*) **1990**, *31*, 377–378.
(5) Tsori, Y.; Tournilhac, F.; Andelman, D.; Leibler, L. *Phys. Rev. Lett.* **2003**, *90*, 1455041–4.
(6) Schmidt, K.; Schoberth, H. G.; Ruppel, M.; Zettl, H.; Hanse, H.; Weiss, T. M.; Urban, V.; Krausch, G.; Boker, A. *Nat. Mater.* **2008**, *7*, 142–145.
(7) Dan, N.; Tirrell, M. *Macromolecules* **1993**, *26*, 637–642.
(8) Cantor, R. *Macromolecules* **1980**, *14*, 1186–1193.
(9) Stepánek, P.; Tuzar, Z.; Nallet, F.; Noirez, L. *Macromolecules* **2005**, *38*, 3426–3431.
(10) Giacomelli, F. C.; Pereira, F. V.; Moussaid, A.; da Silveira, N. P. *Macromol. Symp.* **2006**, *245−246*, 457–462.
(11) Giacomelli, F. C.; Riegel, I. C.; Petzhold, C. L.; da Silveira, N. P. *Macromolecules* **2008**, *41*, 2677–2682.
(12) Giacomelli, F. C.; da Silveira, N. P.; Stepánek, P. *Macromolecules* **2009**, *42*, 3818–3822.
(13) Boker, A.; Elbs, H.; Hansel, H.; Knoll, A.; Ludwigs, S.; Zettl, H.; Zvelindovsky, A. V.; Krausch, G. *Macromolecules* **2003**, *36*, 8078–8087.
(14) Olszowka, V.; Hund, M.; Kuntermann, V.; Scherdel, S.; Tsarkova, L.; Boker, A.; Krausch, G. *Soft Matter* **2006**, *2*, 1089–1094.

(15) Schmidt, K.; Schoberth, H. G.; Schubert, F.; Hansel, H.; Fischer, F.; Weiss, T. M.; Sevink, G. J. A.; Zvelindovsky, A. V.; Boker, A.; Krausch, G. *Soft Matter* **2007**, *3*, 448–453.
(16) Schmidt, K.; Boker, A.; Zettl, H.; Schubert, F.; Hansel, H.; Fischer, F.; Weiss, T. M.; Abetz, V.; Zvelindovsky, A. V.; Sevink, G. J. A.; Krausch, G. *Langmuir* **2005**, *21*, 11974–11980.
(17) Boker, A.; Schmidt, K.; Knoll, A.; Zettl, H.; Hansel, H.; Urban, V.; Abetz, V.; Krausch, G. *Polymer* **2006**, *47*, 849–857.
(18) Xu, T.; Zhu, Y.; Gido, S. P.; Russell, T. P. *Macromolecules* **2004**, *37*, 2625–2629.
(19) Xu, T.; Zvelindovsky, A. V.; Sevink, G. J. A.; Lyakhova, K. S.; Jinnai, H.; Russel, T. P. *Macromolecules* **2005**, *38*, 10788–10798.
(20) Xu, T.; Hawker, C. J.; Russell, T. P. *Macromolecules* **2003**, *36*, 6178–6182.
(21) Tsori, Y.; Andelman, D. *Macromolecules* **2002**, *35*, 5161–5170.
(22) Matsen, M. W. *Macromolecules* **2006**, *39*, 5512–5520.
(23) Pereira, G. G.; Williams, D. R. M. *Macromolecules* **1999**, *32*, 8115–8120.
(24) Xu, T.; Hawker, C. J.; Russell, T. P. *Macromolecules* **2005**, *38*, 2802–2805.
(25) Wang, J.; Leiston-Belanger, J. M.; Sievert, J. D.; Russell, T. P. *Macromolecules* **2006**, *39*, 8487–8491.
(26) Matsen, M. W. *J. Chem. Phys.* **2006**, *124*, 0749061–9.
(27) Xu, T.; Zvelindovsky, A. V.; Sevink, G. J. A.; Gang, O.; Ocko, B.; Zhu, Y.; Gido, S. P.; Russell, T. P. *Macromolecules* **2004**, *37*, 6980–6984.
(28) Boissy, C.; Atten, P.; Foulc, J.-N. *J. Electrostat.* **1995**, *35*, 13–20.
(29) Kimishima, K.; Koga, T.; Hashimoto, T. *Macromolecules* **2000**, *33*, 968–977.
(30) Sota, N.; Hashimoto, T. *Polymer* **2005**, *46*, 10392–10404.
(31) Sakurai, S.; Hashimoto, T.; Fetters, L. J. *Macromolecules* **1996**, *29*, 740–747.
(32) Li, M.; Liu, Y.; Nie, H.; Bansil, R.; Steinhart, M. *Macromolecules* **2007**, *40*, 9491–9502.
(33) Lin, C.-Y.; Schick, M.; Andelman, D. *Macromolecules* **2005**, *38*, 5766–5773.
(34) Pinna, M.; Zvelindovsky, A. V.; Todd, S.; Goldbeck-Wood, G. *J. Chem. Phys.* **2006**, *125*, 1549051–10.
(35) Lyakhova, K. S.; Zvelindovsky, A. V.; Sevink, G. J. A. *Macromolecules* **2006**, *39*, 3024–3037.
(36) Wang, J.-Y.; Chen, W.; Russell, T. P. *Macromolecules* **2008**, *41*, 7227–7231.
(37) Higgins, J. S.; Benoit, H. C. *Polymers and Neutron Scattering*; Clarendon Press: Oxford, 1994; Chapter 6.